

Magnetization of electrodeposited nickel: Role of interstitial carbon

C. O'Reilly, S. Sanvito, F. M. F. Rhen,^{a)} P. Stamenov, and J. M. D. Coey
 Physics Department, Trinity College, Dublin 2, Ireland

(Presented on 1 November 2005; published online 18 April 2006)

The magnetization of nickel foils electrodeposited under different conditions was not usually found to differ significantly from that of the bulk ($55.4 \text{ A m}^2 \text{ kg}^{-1}$). However, some galvanostatically deposited films from a citrate-based electrolyte showed a lower magnetization, which was rose to the bulk value after annealing at 575 K, with no change in lattice parameter. Analysis of the influence of various lattice defects (nickel vacancies or interstitials, hydrogen or carbon impurities) using density functional theory indicates that nickel vacancies may be present in all of the films and that a nonequilibrium concentration of carbon interstitials is the likely explanation of the reduced magnetization in the citrate as-deposited nickel. © 2006 American Institute of Physics.

[DOI: [10.1063/1.2162508](https://doi.org/10.1063/1.2162508)]

Electrodeposition is a popular method for the preparation of magnetic films and multilayers. It was optimized some years ago for Permalloy, $\text{Fe}_{20}\text{Ni}_{80}$, which is widely used in thin film sensors based on anisotropic magnetoresistance.¹ More recently, electrodeposited nanocrystalline Fe-Co-Ni alloys with minimal anisotropy or magnetostriction and a polarization in excess of 2.0 T have been developed for write heads for magnetic recording.² Electrodeposited multilayer Co-Cu stacks,³ segmented nanowires,⁴ and spin valves⁵ all exhibit giant magnetoresistance. Another important use of electrodeposition is to plate the damascene copper interconnects for integrated circuits. These copper deposits are known to evolve in the hours following deposition, when they undergo grain growth, and their electrical conductivity increases by about 20%.⁶

Previous investigations of electrodeposited nickel have indicated a large reduction of Curie temperature from the normal value (628 K), which was attributed to the incorporation of C or Si in the deposits.⁷ Another study, where the deposits were substantially pure, found a reduction of ~ 20 K, which was attributed to the nanocrystalline nature of the films.⁸ It is known that impurity atoms may reduce the magnetization,⁹ but a nanocrystalline structure with a grain size as small as 10 nm was shown to have practically no influence on the magnetization of electrodeposited¹⁰ or gas-condensed¹¹ films, unless the material is oxidized. Electronic structure calculations for a series of relaxed grain boundaries confirmed that magnetic moment is insensitive to the degree of disorder in nickel,¹² showing a reduction of only 15% in the completely amorphous case. On the other hand, a small-angle neutron scattering study of a planar 19.7° grain boundary revealed a substantial increase of nickel moment in a low-density region of half-width 4 nm at the defect.¹³

In the course of an investigation of the magnetization and magnetoresistance of electrodeposited Ni-Cu alloys,¹⁴ we have found that some of these materials had a magnetization that was much lower than it ought to be according to the literature on annealed alloys. Here we focus on pure

nickel in an effort to see if it also has a reduced magnetization and to understand the changes occurring on annealing.

The bright, shiny nickel films were electroplated either galvanostatically (constant current density of 50 mA cm^{-2}) or potentiostatically (at -1.1 V relative to an Ag/AgCl reference electrode) from a standard citrate¹⁵ bath onto rectangular tantalum substrates of area $\approx 0.6 \text{ cm}^2$. Citrate anions act as a complexing agent and buffer the solution keeping the pH at approximately 4.5, avoiding the precipitation of hydroxides. The foils could be peeled from the substrate. They were about $10 \mu\text{m}$ thick, with a mass of approximately 5 mg. X-ray diffraction showed face-centered cubic (fcc) nickel with a 200 texture and lattice parameter $a_0 = 0.3514(5) \text{ nm}$. At this thickness, texture is determined by the deposition current.¹⁶ Heavy element impurities determined by energy-dispersive analysis by X ray (EDAX) are smaller than the limit detection of this technique. The lighter elements O, S, and C were detected using Auger analysis to be below 0.2 and 0.1 at. %, respectively, whereas carbon was present at the 4 ± 3 at. % level in some of the citrate samples.

Magnetization measurements in a superconducting quantum interference device (SQUID) magnetometer of samples deposited potentiostatically from a citrate bath show an average saturation magnetization of $54.6(3) \text{ A m}^2 \text{ kg}^{-1}$ at room temperature ($0.57 \mu_B/\text{Ni}$), which is little different from the accepted room-temperature value for Ni of $55.4 \text{ A m}^2 \text{ kg}^{-1}$ ($0.58 \mu_B/\text{Ni}$). The moment of the galvanostatically deposited samples were more variable, but on heating the samples for 30 min at 575 K there was an increase of magnetization up to $55.9(5) \text{ A m}^2 \text{ kg}^{-1}$, Fig. 1 is an illustration of the one data set. At the same time, there is no change in the lattice parameter [$a_0 = 0.3514(2) \text{ nm}$]. Fitting the x-ray line shapes to pseudo-Voigt profiles indicated that the crystallite size remained about 35 nm both before and after annealing, but there was some reduction in lattice strain after annealing, in agreement with Ref. 17. The nickel films were also prepared at room temperature from sulfate or Watts baths¹⁸ at pH 4.5. Magnetization was $54.9(4)$ and $55.0(3) \text{ A m}^2 \text{ kg}^{-1}$, respectively.

The evolution of the electrodeposits as a function of the temperature was followed in measurements of the ac suscep-

^{a)}Electronic mail: rhenf@tcd.ie

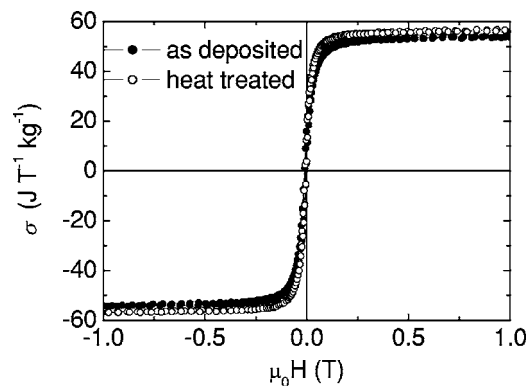


FIG. 1. Magnetization curves of a galvanostatic nickel electrodeposit (a) as prepared and (b) the same sample after heating to 575 K for 30 min.

tibility as shown in Fig. 2. The sample was cycled thrice from 295 to 675 K. Initial cycles took 20 min with the final cycle taking 2 h. On the first cycle, there is an irreversible increase in the real part of the susceptibility χ' (not shown) at about 550 K on heating. The Curie temperature T_C , estimated by extrapolating the imaginary part χ'' to zero, also evolves on thermal cycling from 608 K on first heating to 627 K on the third run, whether heating or cooling. Assuming a thermally activated diffusion process with a diffusion length \sqrt{Dt} of order 15 nm, where $D = \nu a^2 \exp(-\Delta/kT)$ with an attempt frequency $\nu \approx 10^{13}$ due to thermal lattice vibration and an intersite spacing $a \approx 0.2$ nm we estimate the activation energy to be $\Delta \approx 1.1$ eV, supposing the defects diffuse out of a crystallite in about 10 s at 550 K. Scans of resistivity as a function of temperature (shown in Fig. 3) show an irreversible decrease of about 20% when the electrodeposited foils are heated above 575 K. No such decrease was observed for foils deposited from sulfate or Watts baths.

What can be the reason for the changes in the magnetization of electrodeposited nickel brought about by heating to temperatures as low as 550 K, when there is practically no change of lattice parameter? The onset of grain growth in nanocrystalline nickel is above 600 K, although strain release begins at lower temperature.¹³ The recovery of the Curie point on annealing was already noted by Cziráki *et al.*,⁸ but this is not the source of any change in moment in our foils; reducing T_C from 627 to 608 K in itself reduces the room-temperature magnetization by less than 1%. We can

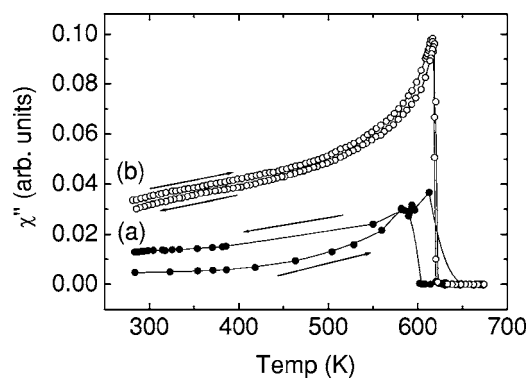


FIG. 2. Magnetic susceptibility measured at 1 kHz for a nickel deposit (a) first heating/cooling cycle and (b) third heating/cooling cycle.

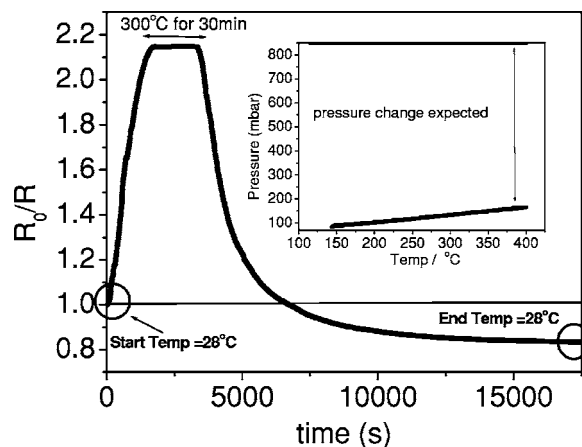


FIG. 3. Change in resistance as nickel electrodeposit is heated and then cooled to room temperature. (Inset) Thermopiezic data showing the absence of hydrogen evolution.

envisage two possibilities: A significant, nonequilibrium concentration of (i) interstitial defects (nickel, hydrogen, carbon) or (ii) substitutional defects (nickel vacancies, carbon, oxygen). Any of these defects may reduce both the nickel moment, and its Curie temperature. Substitutional oxygen, however, would not be expected to anneal out. Grain boundaries leave the moment unchanged, or else increase it.

Interstitial hydrogen seemed the most plausible candidate at first. During electrodeposition, some hydrogen is evolved at the anode, although the current efficiency was high ($>97\%$). Supposing the absorbed hydrogen donates its electron to the nickel d band which contains 0.6 minority-spin holes per atom, the 8% reduction in Ni moment corresponds to a composition of the electrodeposits of $\text{NiH}_{0.05}$. We observed no hydrogen evolution on heating the nickel to 675 K in a thermopiezic analyzer,¹⁹ so an upper limit of 1 at. % can be placed on the hydrogen content. Interstitial hydrogen in metals generally produces a dilation of the lattice. The extra volume per hydrogen²⁰ is 0.6×10^{-30} m³, which means that the lattice parameter should have increased to $a_0 = 0.3518$ nm, which it manifestly did not.

In order to identify the defects responsible, we have studied their effect on the nickel magnetization using density functional theory in the local spin density approximation.²¹ Our numerical implementation is contained in the code SIESTA,²² whose main features are the use of pseudopotentials and a very efficient localized atomic orbital basis set. These enable us to describe large supercells with good accuracy. For this work we consider fcc nickel cells containing 32 sites ($2 \times 2 \times 2$ cubic cells) and a single defect. In our simulations we consider 27 k points in the full cubic Brillouin zone and a basis set containing two basis functions for the 4s and 4p electrons, and three for the 3d. Moreover for most of the defects we allow relaxation. By simple conjugate gradients with a target force of 2×10^{-4} eV \AA^{-1} , using only the gamma point. Finally, the magnetic moment for the relaxed structure is calculated from the relaxed coordinates using 27 k points and the structure is further relaxed if the target force is not matched for this larger k-point sampling.

We first considered the defect to be a nickel vacancy. The calculated moment for the full 32 atom cell was

TABLE I. Calculated change in magnetization and activation energy for diffusion for various defects introduced in a 32 nickel atom cell.

	Δm (μ_B)	$\Delta\sigma/\sigma$ (%)	E_a (eV)
Nickel vacancy	1.08	2.7	1.0
Nickel divacancy	2.09	5.0	0.9
Nickel interstitial	0.85	4.4	0.15 ^a
Carbon substitution	0.81	2.5	—
Hydrogen interstitial	0.60	3.0	0.4 ^b

^aReference 24.^bReference 26.

19.08 μ_B , (0.60 μ_B /atom) whereas for the relaxed 31 atom plus vacancy cell it is 18.00 μ_B , with a reduction of 1.08 μ_B /vacancy. However, σ , the moment per unit mass decreases by less than 3%. Next we investigate whether vacancy complexes can give rise to larger magnetization reduction compared to isolated vacancies. A cell with 30 atoms and a nearest-neighbor vacancy pair returned a drop of moment per unit mass of 5%, similar to two isolated vacancies. The activation energy for the migration of vacancies in Ni in our calculation is $E_m=1.0$ eV to compare with the experimental value for the activation energy for self-diffusion in nickel²³ of 1.42 eV. Our calculations also show that pairwise diffusion reduces this activation energy to about 0.9 eV. A significant vacancy content of order a few percent would be consistent with the observed moments of the foils.

Next consider interstitial nickel. A single nickel interstitial gives a reduction of magnetization of about 40%, but an accurate cell relaxation brings this value to 4.6%. A small concentration of interstitial atoms would be consistent with the observed magnetization but the activation energy for interstitial migration,²⁴ $E_m \approx 0.15$ eV, is so small that these defects would instantly diffuse away at room temperature.

Finally, we examined the effect of interstitial or substitutional carbon. There is negligible equilibrium solubility of carbon in nickel, according to the phase diagram,²⁵ so any carbon-containing phase must be metastable. Experimentally, it is possible to incorporate up to 1.5 at. % by quenching from the melt. The initial moment reduction is 3 μ_B per carbon atom.⁹ Substitutional carbon is calculated to have little influence on the magnetization, reducing the total moment of the 32 atom cell by only 0.81 μ_B . Interstitial carbon, however, is as effective as interstitial nickel at reducing the moment before relaxation. After relaxation the calculated reduction in moment is 1.9 μ_B (see Table I) for a carbon interstitial in the 32-atom cell. Hence no more than 0.5 at. % of interstitial carbon can be present in the potentiostatically deposited films, although the concentration in some galvanostatically deposited films may be higher. The activation energy for diffusion is estimated²⁶ as 1.4 eV, which is consistent with our annealing data. Since hydrogen has been ruled out experimentally, the only defects we have found to be capable of explaining a significant moment reduction are interstitial carbon or nickel vacancy pair. The Auger analysis is consistent with the presence of carbon at the 3 at. % level in some of the as-deposited galvanostatic citrate films.

In conclusion, we have measured no significant reduction in the magnetization of nickel films prepared by poten-

tiostatic electrodeposition, but there is a slight reduction of Curie temperature and moment of films deposited galvanostatically from citrate bath. Normal magnetic properties are restored after briefly heating above 525 K. An analysis of potential defects using density functional theory to calculate their influence on the nickel magnetization leads us to conclude that single nickel vacancies have little influence on the magnetization per unit mass, but carbon interstitials can produce significant reductions. Transient concentrations of non-equilibrium vacancies and interstitials may be expected in other electrodeposited fcc metals, such as copper.

This work forms part of the CINSE project, funded by Science Foundation Ireland. The authors would like to thank Dr. C. Anderson and Professor N. Brown from the University of Ulster for the auger analysis.

- ¹R. L. Comstock, *Introduction to Magnetism and Magnetic Recording* (Wiley, New York, 1999).
- ²T. Osaka, M. Tabai, K. Hayashi, M. Saito, and K. Yamada, *Nature* (London) **392**, 796 (1998).
- ³G. Nabouyouni and W. Schwarzacher, *J. Magn. Magn. Mater.* **156**, 355 (1996).
- ⁴K. Lui, K. Nagodawithana, P. C. Searson, and C. L. Chein, *Phys. Rev. B* **51**, 7381 (1995).
- ⁵K. Attenborough, H. Boeve, J. De Boeck, G. Borghs, and J. P. Celis, *Appl. Phys. Lett.* **74**, 2206 (1999).
- ⁶J. M. E. Harper, C. Cabral Jr., P. C. Andricacos, L. Gignac, I. C. Noyan, K. P. Rodbell, and C. K. Hu, *J. Appl. Phys.* **86**, 2516 (1999).
- ⁷M. Y. Popereka, *J. Electrochem. Soc.* **122**, 92 (1975).
- ⁸A. Cziráki, Zs. Tonkovic, I. Geröes, B. Fogarassy *et al.*, *Mater. Sci. Eng., A* **179–180**, 531 (1994).
- ⁹M. C. Cadeville and C. Lerner, *Philos. Mag.* **33**, 801 (1976).
- ¹⁰M. J. Aus, B. Szpunar, A. M. El-Sherik, U. Erb *et al.*, *Scr. Metall. Mater.* **27**, 1639 (1992).
- ¹¹H. Kirker, H. Kronmüller, H. E. Schaefer, and T. Suzuki, *J. Appl. Phys.* **79**, 5143 (1996).
- ¹²B. Szpunar, U. Erb, G. Palumbo, K. T. Aust, and L. J. Lewis, *Phys. Rev. B* **53**, 5547 (1996).
- ¹³M. R. Fitzsimmons, A. Röhl, E. Burkel, K. E. Sickafus *et al.*, *Nanostruct. Mater.* **6**, 539 (1995).
- ¹⁴Cora O'Reilly, Ph.D. thesis, Trinity College, Dublin, Ireland, 2003.
- ¹⁵Electrodeposition bath: 1.14 M NiSO₄–6H₂O; 0.2 M C₆H₅Na₃O₇–2H₂O; 0.034 M NaCl, pH 4.5. Films were deposited potentiostatically at –1.1 V relative to Ag/AgCl for 600 s and also galvanostatically at the corresponding current density –50 mA/cm² for 600 s. A concentric nickel ring anode and the deposition temperature was 50 °C.
- ¹⁶V. M. Koslov and L. Peraldo, *Mater. Chem. Phys.* **77**, 289 (2002).
- ¹⁷J. A. Eastaman, M. A. Beno, G. S. Knapp, and J. L. Thompson, *Nanostruct. Mater.* **6**, 543 (1995).
- ¹⁸Sulfate bath: 1.14 M NiSO₄–6H₂O, 0.04 M H₃BO₃, pH 4.5 and Watts bath: 1.14 M NiSO₄–6H₂O, 0.15 M NiCl₂–6H₂O, 0.65 M H₃BO₃, pH 4.5. Films were electrodeposited potentiostatically at –1.0 V relative to Ag/AgCl for 600 s.
- ¹⁹D. H. Ryan and J. M. D. Coey, *J. Phys. E* **19**, 693 (1986).
- ²⁰*Hydrogen in Metals I: Basic Properties*, edited by G. Alefeld and J. Völkl (Springer, Berlin, 1978) p. 53.
- ²¹H. Hohenberg and W. Kohn, *Phys. Rev.* **136**, B864 (1964); W. Kohn and L. J. Sham, *ibid.* **140**, A1133 (1965).
- ²²J. M. Soler, E. Artacho, J. D. Gale, A. García, J. Junquera, P. Ordejón, and D. Sánchez-Portal, *J. Phys.: Condens. Matter* **14**, 2745 (2002).
- ²³M. E. Glicksman, *Diffusion in Solids* (Wiley, New York, 2000).
- ²⁴Landolt Bornstein, *Numerical Data and Functional Relationships in Science and Technology New Series*, edited by W. Martienssen and Y. Itikawa (Springer, New York, 1961).
- ²⁵T. B. Massalski, *Binary Alloy Phase Diagrams* (ASM International, Materials Park, OH, 1990), Vol 1.
- ²⁶R. J. Borg and G. J. Dienes, *An Introduction to Solid State Diffusion* (Academic, San Diego, CA, 1988).